Supplemental Information

Chemical and electronic structure of the heavily intermixed (Cd,Zn)S:Ga/CuSbS₂ interface

C. Hartmann[1], R. E. Brandt[2], L. L. Baranowski[3,4], L. Köhler[1], E. Handick[1], R. Félix[1], R. G. Wilks[1,5], A. Zakutayev[3], T. Buonassisi[2], and M. Bär[1,5,6,7]

[1]Helmholtz-Zentrum Berlin für Materialien und Energie GmbH (HZB), Berlin, Germany
[2]Massachusetts Institute of Technology (MIT), Cambridge, Massachusetts, U.S.A.
[3]National Renewable Energy Laboratory, Golden, Colorado 80401, United States
[4]Physics Department, Colorado School of Mines, Golden, Colorado 80401, United States
[5]Energy Materials In-Situ Laboratory Berlin (EMIL), HZB, Berlin, Germany
[6]Helmholtz-Institute Erlangen-Nürnberg for Renewable Energy (HI ERN), Berlin, Germany
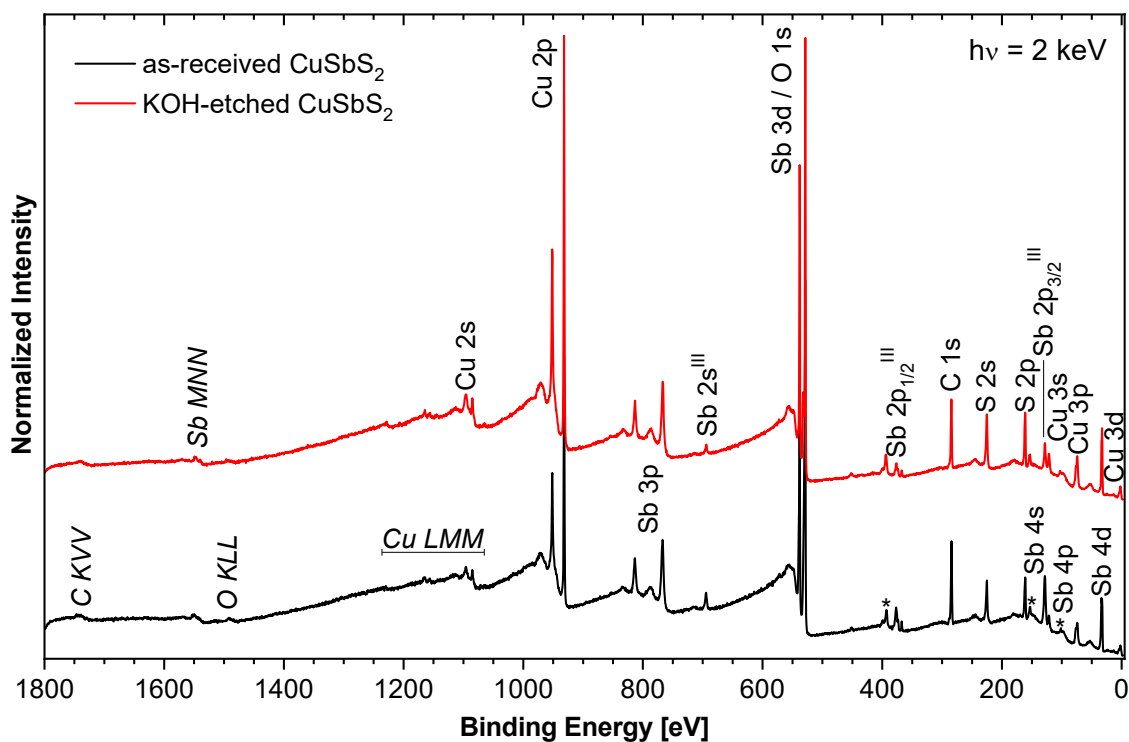[7]Friedrich-Alexander-Universität Erlangen-Nürnberg, Erlangen, Germany

Figure S1: HAXPES survey spectra (recorded with 2 keV) of an as-received CuSbS₂ absorber and of an absorber that was subject to a KOH-etch step. Spectra normalized to Cu 2p₃/₂ intensity. A vertical offset was added for clarity. The lines with a numeral III superscript (i.e., Sb 2sᴵᴵᴵ) are excited by photons resulting from third order monochromator diffraction.
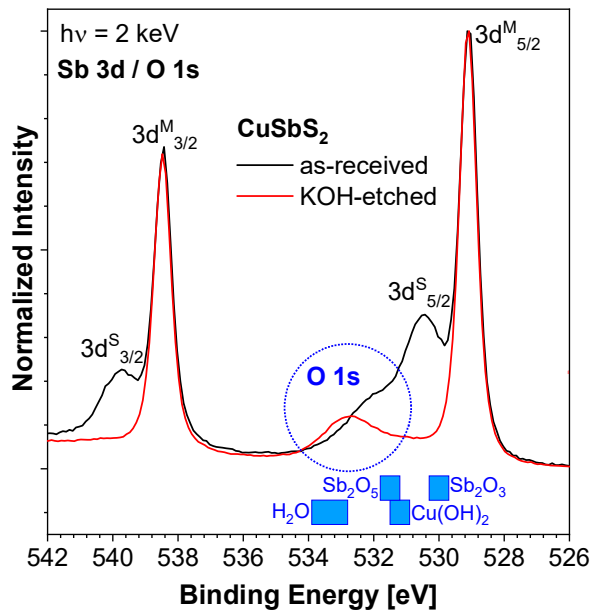
Figure S2: Normalized HAXPES detail spectra of the overlapping region of the Sb $3d_{5/2}$ and $3d_{3/2}$ and of the O 1s lines of an as-received and KOH-etched $CuSbS_2$ absorber. Some O 1s reference position ranges of relevant compounds[1,2] are added as blue boxes for comparison.

For the as-received $CuSbS_2$ absorber we find two distinct contributions to the Sb $3d_{5/2}$ and $3d_{3/2}$ lines: The main peaks $3d^M_{5/2}$ and $3d^M_{3/2}$ at 529.1 and 538.5 eV, respectively, and the secondary contributions $3d^S_{5/2}$ and $3d^S_{3/2}$ at 530.5 eV and 539.9 eV, respectively. This agrees with the main contribution assigned to Sb in a $CuSbS_2$ environment and the secondary contribution attributed to Sb in a SbO_x environment,[1,2] corroborated by the respective O 1s line. Upon KOH-etching the secondary contributions to the Sb 3d lines disappear and the O 1s peak is reduced in intensity. In parallel, the center of mass of the O 1s peak shifts to higher binding energies (BE). The comparison of the energetic position of O 1s peak of the KOH-etched $CuSbS_2$ spectrum with the given reference position ranges suggests a significant part of the observed oxygen being attributed to (adsorbed) water and/or OH groups formed during the KOH etching.
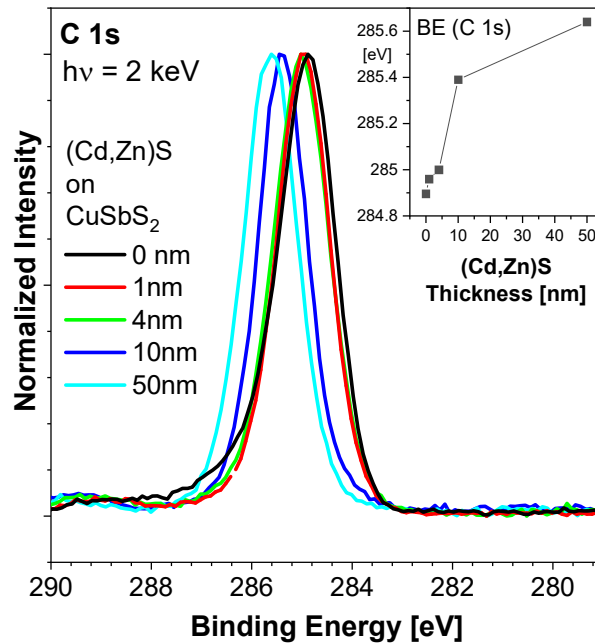
Figure S3: Normalized HAXPES C 1s detail spectra (recorded with 2 keV) of the bare CuSbS$_2$ absorber ("0 nm") and of the (Cd,Zn)S:Ga/CuSbS$_2$ samples with buffer thicknesses varying from 1 nm to 50 nm. Inset: C 1s binding energies (BE) as a function of buffer layer thickness.

With increasing buffer layer thickness a C 1s shift from 284.9 eV (for the bare absorber ≡ "0 nm (Cd,Zn)S Thickness") to 285.6 eV (for the 50 nm (Cd,Zn)S:Ga/CuSbS$_2$ sample) is observed (see inset of Figure S3). The most pronounced shift is seen for the two thickest buffer layer samples (10 and 50 nm (Cd,Zn)S:Ga). Hence, for these two samples we assume charging to significantly influence the energetic position of the recorded HAXPES spectra.
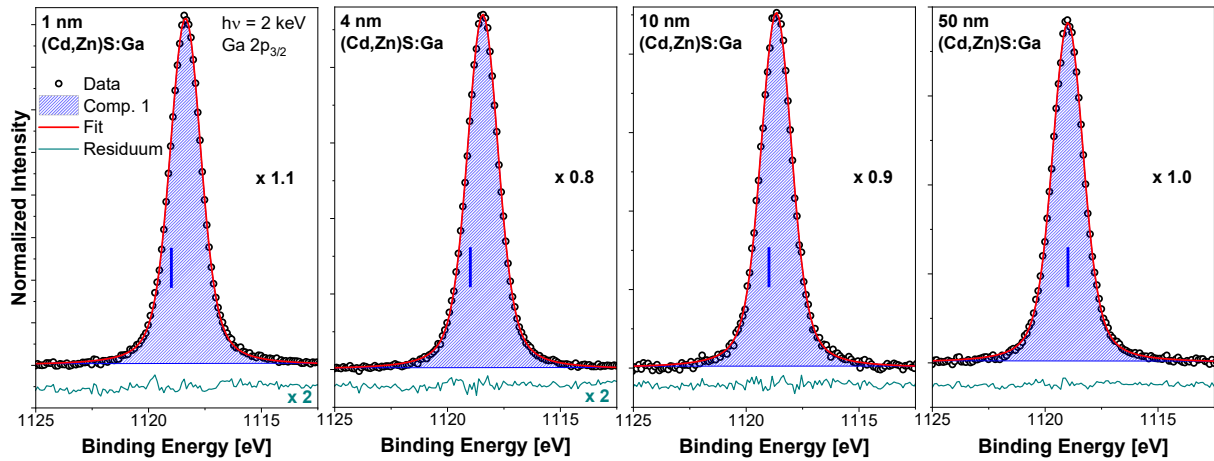
Figure S4: Ga 2p$_{3/2}$ HAXPES detail spectra recorded with 2 keV of the (Cd,Zn)S:Ga/CuSbS$_2$ samples with buffer thicknesses varying from 1 nm (leftmost panel) to 50 nm (rightmost panel). Spectra have been normalized to the background at low BE. The background subtracted data is shown together with the fits and resulting residuals (i.e., [data − fit] - shown on different scale if required with scaling factor indicated as e.g., x 0.5). Additionally, the magnification factors are stated (as e.g., x 1.0) that were applied to show all spectra on the same intensity scale as that of the 50 nm (Cd,Zn)S:Ga/CuSbS$_2$ sample. The vertical blue line indicates the BE position of the peak location in the spectrum the thickest buffer sample.
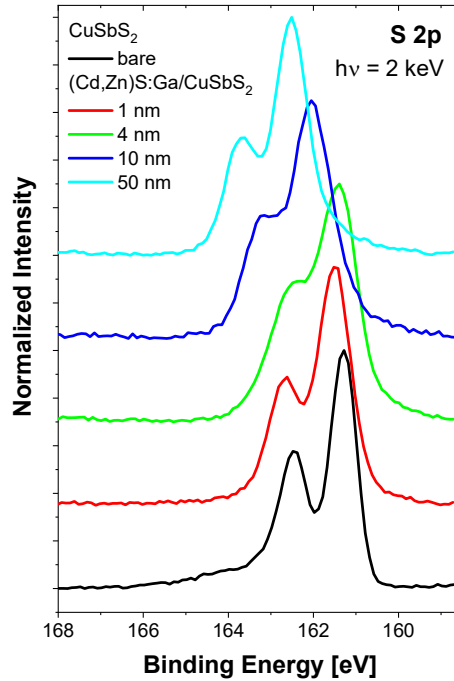
Figure S5: Normalized HAXPES S 2p detail spectra (recorded with 2 keV) of the bare CuSbS$_2$ absorber (bottommost spectrum) and of the (Cd,Zn)S:Ga/CuSbS$_2$ samples with buffer thicknesses varying from 1 nm (spectrum second from the bottom) to 50 nm (topmost spectrum). A vertical offset was added for clarity.

S is present in the CuSbS$_2$ absorber, as well as in the (Cd,Zn)S:Ga buffer layer, resulting in a complex interplay of different spectral features in close energetic proximity. We find the S 2p spectra shifted to higher BE with increasing buffer layer thickness (most probably caused by increasingly pronounced sample charging) and a varying width of the S 2p$_{3/2}$ and 2p$_{1/2}$ contributions reaching its maximum at intermediate (4 and 10 nm) buffer layer thicknesses with the S 2p spectrum of the bare absorber exhibiting the narrowest line shape. This is most clearly visible by observing the changing depth of the local intensity minima between the 2p$_{3/2}$ and 2p$_{1/2}$ contributions (see Figure S5). In addition, the energy window of the S 2p spectra also contains Ga 3s contributions (at approximately 161 eV BE) that are significantly lifetime broadened and thus further complicate the fit analysis of the S 2p region. Hence, we deliberately refrain from fitting this region.

Table S1: Considered core levels with their binding energy (BE) and kinetic energy (KE) considering an excitation energy of 2003 eV together with the corresponding electron analyzer transmission (T), photoionization cross section (σ),[3,4] and photoelectron's inelastic mean free path (IMFP) in $Cd_{0.8}Zn_{0.2}S$.[5]

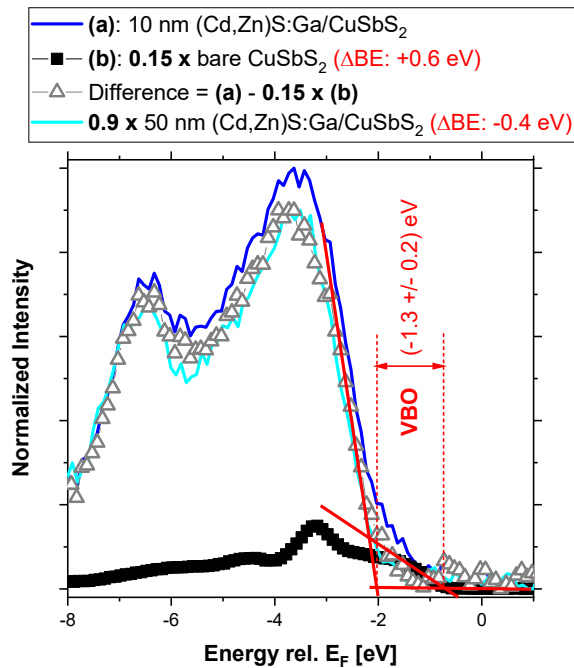| Core level	BE (eV)	KE (eV)	T (eV)	σ (kB)	IMFP (nm)
Sb $3d_{3/2}$	537	1466	0.746	130.485	2.85
Cu $2p_{3/2}$	933	1070	0.806	226.113	2.38
Zn $2p_{3/2}$	1022	981	0.820	261.692	2.23
Ga $2p_{3/2}$	1117	886	0.836	301.313	2.09
Cd $3d_{5/2}$	405	1598	0.727	131.737	3.07

Figure S6: Visualization of subtracting the (properly scaled and shifted) spectrum of the bare CuSbS$_2$ absorber (b) from the 10 nm (Cd,Zn)S:Ga/CuSbS$_2$ spectrum (a), resulting in a difference spectrum, representing the buffer related contribution to the VB spectrum. For comparison the (properly scaled and shifted) spectrum of the 50 nm Cd,Zn)S:Ga/CuSbS$_2$ sample is shown. The linear extrapolation of the leading edges of the (scaled and shifted) spectrum of the bare absorber and of the difference spectrum to derive the VBO is also depicted.

For a reasonable difference spectrum, the absorber spectrum had to be properly scaled (by a factor of 0.15) and shifted away from E$_F$ (ΔBE = +0.6 eV). Then the derived difference resembles the (properly scaled [x 0.9] and shifted [ΔBE = -0.4 eV]) spectrum of the 50 nm (Cd,Zn)S:Ga/CuSbS$_2$ sample quite well. By computing the difference of the VBM (obtained by linear extrapolation of the leading edge of the spectrum, see red lines in the left panel of Figure S6) of the difference spectrum (representing now the buffer related contribution to the spectrum of the 10 nm (Cd,Zn)S:Ga/CuSbS$_2$ sample) and the VBM of the properly scaled and shifted spectrum of the bare absorber, we derive the VBO at the (10 nm) buffer/absorber interface to be (-1.3 ± 0.2) eV.

HAXPES information depth

The HAXPES information depth is governed by the inelastic mean free path (IMFP) of the photoelectrons. For 2 keV excited Cu $2p_{3/2}$ photoelectrons the IMFP is approximately 2.4 nm in (Cd,Zn)S.[5] Usually the information depth is considered to be 3 x IMFP. In that case, 95% of the (from the sample surface exponentially decreasing signal) has been collected.

REFERENCES

(1) Whittles, T. J.; Veal, T. D.; Savory, C. N.; Welch, A. W.; de Souza Lucas, F. W.; Gibbon, J. T.; Birkett, M.; Potter, R. J.; Scanlon, D. O.; Zakutayev, A.; Dhanak, V. R. Core Levels, Band Alignments, and Valence-Band States in CuSbS2 for Solar Cell Applications. ACS Appl. Mater. Interfaces **2017**, 9 (48), 41916–41926. https://doi.org/10.1021/acsami.7b14208.

(2) *Wagner, C. D. The NIST X-Ray Photoelectron Spectroscopy (XPS) Database. 76.*

(3) Trzhaskovskaya, M. B.; Nefedov, V. I.; Yarzhemsky, V. G. Photoelectron Angular Distribution Parameters for Elements Z=1 TO Z=54 in the Photoelectron Energy Range 100–5000 eV. *At. Data Nucl. Data Tables* **2001**, *77* 8(1), 97–159. https://doi.org/10.1006/adnd.2000.0849.

(4) Trzhaskovskaya, M. B.; Nefedov, V. I.; Yarzhemsky, V. G. Photoelectron Angular Distribution Parameters for Elements Z=55 TO Z=100 in the Photoelectron Energy Range 100–5000 eV. *At. Data Nucl. Data Tables* **2002**, *82* (2), 257–311. https://doi.org/10.1006/adnd.2002.0886.

(5) QUASES-IMFP-TPP2M - QUASES http://www.quases.com/products/quases-imfp-tpp2m/ (accessed Nov 30, 2020).